NASA TECHNICAL TRANSLATION

NASA TT F-14,717

QUASI-STATIC OSCILLATIONS IN THE ATMOSPHERE OF η AQUILAE

P. Ledoux and J. Grandjean

Translation of: "Oscillations quasi-statiques dans l'atomosphere de Aquilae", Academies Royale De Belgiques, Ser. 5, Vol. 41, 1955, 29 pp.

NATIONAL AERONAUTICS AND SPACE ADMINISTRATION
WASHINGTON, D.C. 20546
NOVEMBER 1972

ASTROPHYSICS

QUASI-STATIC OSCILLATIONS IN THE ATMOSPHERE OF η AQUILAE

P. Ledoux* and J. Grandjean**

ABSTRACT: The variation with phase of the properties of hydrostatic atmospheric models constructed to interpret the observations of η Aquilae are discussed from the point of view of the theory of pulsations. The lagrangian variations of density combined with the equation of continuity (conservation of mass) yield a distribution of velocity with depth which is compatible with the observations. /1010***

The conservation of energy is satisfied within the precision of the numerical integrations used.

In the case of the equation of motion (conservation of momentum) the problem arises of interpreting the small values of the effective gravity g_e adopted in the models. This difficulty which is not bound up with pulsations is discussed at some length. The hypothesis of very strong convection currents arising in the ionization zone of hydrogen and carrying an appreciable net flux of momentum across the photosphere holds some promise of explaining the weak g_e, the atmosphere being then composed of large elements nearly in free fall. The combination of this hypothesis with the theory of pulsations is a delicate problem and a qualitative discussion only is given.

1. INTRODUCTION

The atmosphere models, which have served for discussing the continuous background of η Aquilae [1] and the observed differential velocities [2], have deen derived on the basis of the usual theory of hydrostatic and radiative equilibrium, with the relaxation time of the radiation field being assumed much shorter than the pulsation period and with the acceleration due to the pulsation being incorporated implicitly in the effective gravity ge. /1011

If one assumes the validity of this quasi-static hypothesis, one can, from the comparison between the models for the different phases, determine the variations of the various parameters and ascertain if they are compatible with the dynamic and thermodynamic theory.

Since a complete description of these models has been published elsewhere [2], we will repeat in Table I only those of their characteristics that are essential to the discussion.

---

*Member of F. N. R. S.

**Introduced by P. Swings.

***Numbers in the margin indicate pagination in the foreign text.

TABLE I

	Phase 0,0				Phases 0,15 and 0,90				Phases 0,35 and 0,85				Phases 0,556 and 0,75				Phase 0,68			
	$T_e = 5730°$; $\log g_e = 0,4$				$T_e = 5400°$; $\log g_e = 0,35$				$T_e = 5200°$; $\log g_e = 0,3$				$T_e = 4880°$; $\log g_e = 0,175$				$T_e = 4800°$; $\log g_e = 0$			
τ	$\log \varkappa$	$\rho\, 10^{10}$	$h\, 10^{-11}$ cm	$m(h)$ gr	$\log \varkappa$	$\rho\, 10^{10}$	$h\, 10^{-11}$ cm	$m(h)$ gr	$\log \varkappa$	$\rho\, 10^{10}$	$h\, 10^{-11}$ cm	$m(h)$ gr	$\log \varkappa$	$\rho\, 10^{10}$	$h\, 10^{-11}$ cm	$m(h)$ gr	$\log \varkappa$	$\rho\, 10^{10}$	$h\, 10^{-11}$ cm	$m(h)$ gr
0,01	-3,03	1,35	2,13	14	-3,15	1,12	2,50	12	-3,20	1,41	2,41	17	-3,28	1,77	3,02	27	-3,25	1,85	4,36	40
0,03	-2,80	3,28	2,85	35	-2,83	3,62	3,38	40	-2,88	4,00	3,28	48	-2,98	4,27	3,96	65	-3,05	3,45	5,45	77
0,06	-2,66	4,99	3,24	54	-2,59	5,38	3,77	61	-2,73	5,80	3,67	71	-2,80	6,10	4,43	93	-2,87	4,91	6,12	110
0,10	-2,58	6,61	3,53	72	-2,62	7,02	4,06	80	-2,64	7,44	3,97	92	-2,72	7,69	4,78	119	-2,78	6,11	6,61	140
0,20	-2,40	9,80	3,92	110	-2,47	10,35	4,47	122	-2,48	10,62	4,38	136	-2,56	10,88	5,26	174	-2,63	8,49	7,31	200
0,30	-2,25	11,73	4,12	135	-2,40	12,47	4,74	151	-2,43	12,62	4,62	166	-2,48	12,83	5,55	211	-2,56	10,00	7,74	243
0,40	-2,15	12,93	4,25	153	-2,30	14,19	4,88	176	-2,37	14,31	4,81	193	-2,42	14,29	5,76	241	-2,50	11,24	7,98	279
0,60	-1,95	14,63	4,42	181	-2,15	16,68	5,10	216	-2,25	17,09	5,07	240	-2,33	16,68	6,06	293	-2,42	13,21	8,46	343
1,00	-1,55	16,28	4,58	217	-1,80	19,65	5,32	273	-2,00	20,71	5,36	311	-2,18	20,15	6,45	379	-2,32	16,12	9,10	447
1,40	-1,23	16,31	4,64	231	-1,50	20,52	5,42	298	-1,70	22,12	5,51	351	-2,00	22,17	6,70	440	-2,13	18,30	9,51	531
1,80	-0,95	16,00	4,67	238	-1,29	20,21	5,47	310	-1,48	22,32	5,58	371	-1,81	23,10	6,84	480	-1,95	19,06	9,77	591
2,50	-0,65	15,28	4,70	244	-0,92	19,64	5,52	324	-1,10	22,06	5,64	392	-1,46	23,72	6,98	525	-1,62	19,90	10,00	653
3,20	-0,38	14,19	4,72	248	-0,67	18,89	5,54	330	-0,85	21,27	5,68	401	-1,18	23,37	7,05	545	-1,35	19,80	10,11	682
4,00	-0,08	13,26	4,73	250	-0,43	18,07	5,56	335	-0,60	20,43	5,70	406	-0,93	22,51	7,09	557	-1,10	19,50	10,19	700
5,00	+0,22	12,14	4,74	251	-0,10	16,88	5,57	337	-0,34	19,11	5,71	410	-0,70	21,37	7,12	566	-0,80	18,50	10,23	713
6,00	+0,40	11,24	4,74	252	+0,15	15,80	5,57	339	-0,07	18,15	5,72	412	-0,45	20,36	7,14	571	-0,60	17,90	10,26	719

2. VARIATIONS IN THE DENSITY ρ AND IN THE AVERAGE ABSORPTION COEFFICIENT $\bar{\kappa}$

Interpolation in Table I allows one to determine the variations of ρ and $\bar{\kappa}$ for either a constant optical depth $\bar{\tau}_0$ or a constant geometrical depth h_0, or even with respect to an element of matter (variations in the Lagrangian sense) characterized by the constant mass m(h) which it supports. Since these latter variations are the most interesting physically, we have repeated them in Table II and Fig. 1 for three elements supporting, respectively, 72, 135 and 181 grams and which occupy, in the phase 0.0, the optical depths $\bar{\tau} = 0.1$, 0.3 and 0.6, respectively.

TABLE II. DENSITY VARIATIONS OF AN ELEMENT OF MATTER

M\phase	0,00	0,15	0,35	0,556	0,68	0,75	0,85	0,90
72	6,61	6,35	5,95	4,75	3,25	4,75	5,95	6,35
135	11,73	11,35	10,50	8,64	5,94	8,64	10,50	11,35
181	14,63	14,45	13,56	11,28	7,75	11,28	13,56	14,45

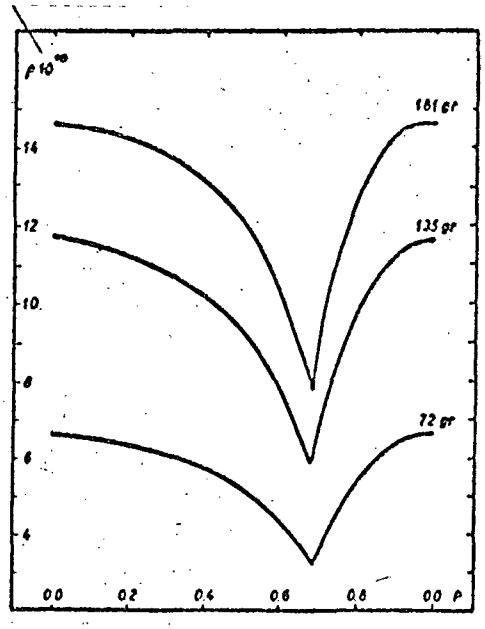

Fig. 1. Lagrangian variations of the density ρ of three particles.

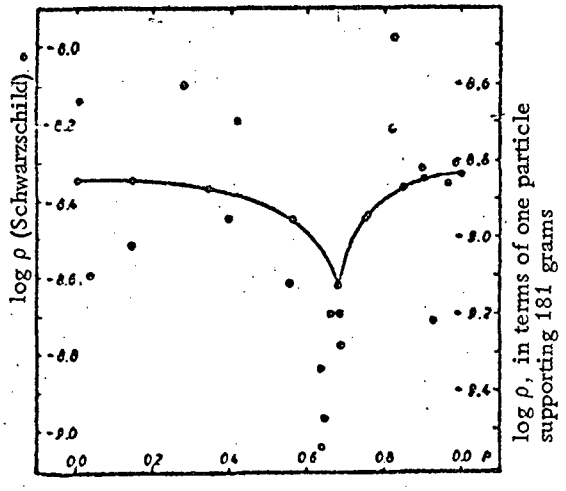

Fig. 2. Comparison between our Lagrangian variation of the density (points) and that obtained by Schwarzschild from a study of the absoprtion lines (small circles). The ordinate scales have been shifted to facilitate the comparison.

It is seen that for these three levels the Lagrangian variation of the density is, for the most part, in phase with the radial velocity and that the only marked difference from one

level to another is in the amplitude.

Figure 2 presents a comparison between the variation of ρ obtained by us and that obtained by W. S. Adams, M. Schwarzschild and B. Schwarzschild [3] from a study of the absorption lines. It proves that the two variations have nearly the same behavior, to within a small factor due to the lower g_e adopted by us.

The same can be said about the comparison of the variations of the average absorption coefficient illustrated by Fig. 3.

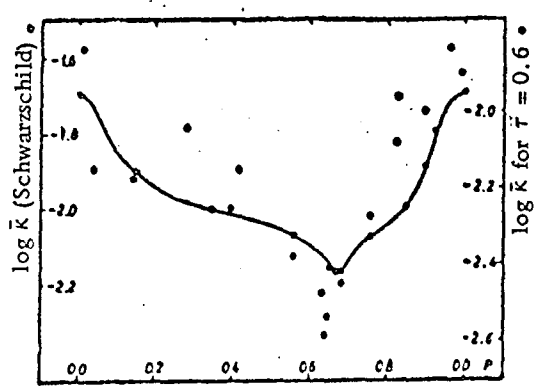

Fig. 3. Comparison between our variation of $\bar{\kappa}$ (points) and that of Schwarzschild (small circles) after shift of ordinate scales.

3. EQUATION OF MOTION AND THE EFFECTIVE GRAVITY g_e

Normally, the equation of motion

$$\frac{d^2r}{dt^2} = -g - \frac{1}{\rho}\frac{dP}{dr} \qquad (1)$$

should provide a dynamic test, with the pressure gradient being taken from the models and the acceleration from the observed radial velocities.

But it is a well-known fact [3 to 8] that for all the phases the effective gravity $g_e = -dP/\rho dr$ obtained from the line spectrum is much smaller than the dynamic gravity $g_d = GM/R^2 + d^2r/dt^2$.

This is also true in our models, where g_e is primarily determined via the Balmer discontinuity (Table III). Nevertheless, recently Canavaggia and Pecker [9], as well as Whitney [10] have obtained by the same method very much higher g_e values, higher, in fact, than g_d. The source of this discrepancy must be the higher temperatures assumed by these authors, and the different methods employed to evaluate the flux on both sides of the Balmer discontinuity. Not wishing to discuss here the respective merits of either solution, we feel, nevertheless, that on the whole more of the evidence favors the low g_e.

TABLE III. COMPARISON BETWEEN g_e, GM/R^2 AND THE ACCELERATION OBTAINED FROM THE RADIAL VELOCITIES

Phases	g_e	$g = GM/R^2$	dV/dt	Phases	g_e	$g = GM/R^2$	dV/dt
0,00	2,5	46	— 1	0,68	1	43	— 23
0,15	2,2	42	— 12	0,75	1,5	46	— 3
0,35	2,0	40	— 8	0,85	2,0	49	— 68
0,556	1,5	41	— 22	0,90	2,2	49	+ 61

Since this effect is not limited to the cepheids [5, 6, 11], its cause should not be sought in the pulsation.

In order to explain these low g_e, Pannekoek [5, 8] proposed introducing into these atmospheres a velocity field that increases outward. It is assumed to be created by a "total gravity" that becomes negative in the upper layers. But this hypothesis leads to a continuous expansion at appreciable rates, the existence of which has not been confirmed by observation and the theoretical justification of which is difficult.

More often, one resorts to employment of a very pronounced "turbulence" which, in all these atmospheres, shows up in the growth curves and again in the line profile. For example, Adams and Schwarzschild [3] have obtained average turbulence velocities of the order of 4 and 12 km/sec by the two methods in the atmosphere of η Aquilae, at an average line formation level of $\bar{\tau} = 0.3$. /1016

The argument rests on the Reynolds pressure concept, which reduces, in the isotropic turbulence case, to a pressure which we designate by $P_t = (1/3)\rho\bar{C}^2$, where $\bar{C}^2$ is the mean square velocity of the turbulent elements. In this case, ignoring radiation pressure, Eq. (1) becomes

$$-\frac{1}{\rho}\frac{\partial P_o}{\partial r} = g_e = g + \frac{d^2r}{dt^2} + \frac{1}{\rho}\frac{\partial P_t}{\partial r}. \qquad (2)$$

Usually, the discussion is based on Eq. (2), integrated for an isothermal atmosphere with $\bar{C}^2$ constant. This corresponds to replacing the usual scale factor $RT/\bar{\mu}g$ by $[RT/\bar{\mu} + \bar{C}^2/3]\,g$, or to introducing an effective gravity $g'_e = g/(1 + \bar{C}^2/\bar{c}^2)$, where $\bar{c}^2$ represents the mean square thermal agitation velocity.

For example, with $\bar{C}^2 \simeq 12$ km/sec and $\bar{c}^2 \simeq 7$ km/sec ($T \simeq 5000°$ K, $\bar{\mu} = 1.5$), $g'_e = g/4 \simeq 10$ cm/sec^2, which is still 4 to 5 times higher than the g_e used by us.

Equation (2), on the other hand, shows that more generally g_e tends to become smaller as the rate of decrease of P_t toward the outside increases. In our models, if one interprets the value of $\Delta P_t/\Delta r$ required to explain the low g_e in terms of the change of $\bar{C}$ between $\bar{\tau} = 0.3$ ($\bar{C} \simeq 4$ to 12 km/sec) and the top of the hydrogen instability zone, one finds that at this level $\bar{C} \simeq 30$ km/sec. In spite of the extremely high convection in these regions of very low density, it is doubtful that such rates can ever be attained.

In addition, it appears very difficult to justify such a rapid variation of the kinetic energy of turbulence. This variation must be of the same order as the difference in the potential energy of gravity between the two levels and equal to several times the thermal agitation energy.

The model recently calculated by P. Dumezil-Curien [12] for $g = 32.5$ cm/sec^2 and $k = 4.5$ can serve to make these considerations a little more precise. It contains an extended convective zone beneath the photosphere. The kinetic energy acquired by a unit element of mass in traversing this region of instability is given, in a first approximation, by /1017

$$\frac{1}{2}v_1^2 - \frac{1}{2}v_0^2 = -\int_0^1 \left(g + \frac{1}{\rho}\frac{d\bar{P}}{dr}\right) dr, \tag{3}$$

where the barred symbols denote the average value of the variable in the surrounding medium. Let us direct the discussion to the case of an element moving upward. If, on the average, hydrostatic equilibrium exists, $d\bar{P}/dr = -g\bar{\rho}$, and if one ignores P_t, Eq. (3) can be written as

$$\frac{1}{2}v_1^2 - \frac{1}{2}v_0^2 = \int_0^1 g\left(\frac{\bar{\rho}}{\rho} - 1\right) dr = -\int_{P_0}^{P_1} \frac{R}{\mu}\left(T - \bar{T}\right) d\ln\bar{P}, \tag{4}$$

where T is given by

$$\ln(T/T_0) = \int_{P_0}^{P_1} \frac{\Gamma_2 - 1}{\Gamma_2} d\ln\bar{P} \tag{5}$$

when the motion is considered to be adiabatic.

Although the Γ_2 of Eq. (5) refers to the moving element, we have used the Γ_2 value calculated by P. Dumezil-Curien for the ambient medium. This does not cause a serious error at the start of the motion, but at the top of the unstable region and in the bottom layers of the radiative atmosphere Γ_2 will tend to remain appreciably smaller in the upward-moving element than in the ambient medium, which would tend to lengthen the period of computed positive acceleration. The kinetic energies calculated in this manner can therefore be considered, in this sense, as the lower limits. On the other hand, however, the viscosity and the radiative conduction tend to diminish the velocities of these flows; and besides, if they attain supersonic velocities, it may happen that the losses via shock waves would increase considerably. /1018

The integrand of Eq. (4) is shown in Fig. 4, which also gives the variation of $1/2v_1^2$, with v_0 assumed to be zero. It shows that at the top of the unstable zone (log P = 3.470, $\bar{\tau} = 1.04$), $1/2v_1^2 \simeq 10^{12}$ or $v_1 \simeq 14$ km/sec. At this point, however, T is still much higher than $\bar{T}$ and v_1 will continue to increase until $\bar{\tau} = 0.03$ (log P $\simeq$ 2.625), where it reaches a value of the order of 16 km/sec. Let us note that such an element, considered to be in free fall after leaving this point, can rise above the normal atmosphere of P. Dumezil-Curien's mode to a height of the order of the thickness of this atmosphere. /1019

It is evident that such flows, with which it is reasonable to associate the high velocities of the order of 12 km/sec observed in the line profile, can alter the structure of the outer layers considerably. Certainly, the concept of turbulence pressure loses all meaning in this case. However, the momentum flux due to these flows can ensure a dynamic support of the atmosphere that becomes more efficient as the cross sections of the rising flows become smaller and acquire higher velocities than the descending

flows (with mass conservation being preserved, of course).

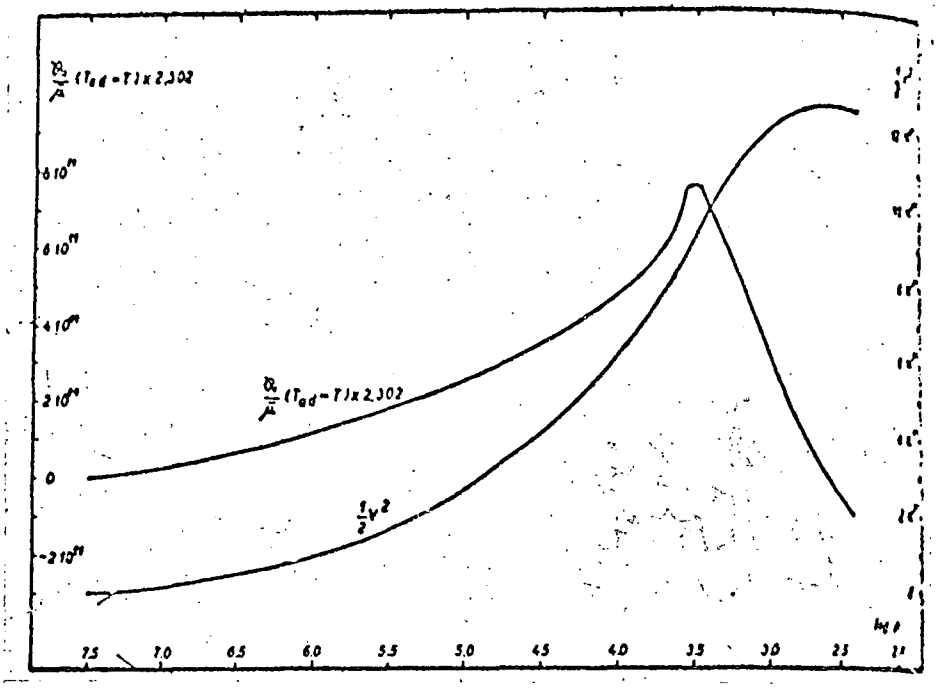

Fig. 4. Variation of the kinetic energy of an element through the outer layers of the Dumezil-Curien model.

Pushing this point of view to the extreme, the atmosphere, distended to well beyond the normal dimensions of a hydrostatic atmosphere, is then reduced to an ensemble of nearly independent, rapidly moving elements [13]. Of course, this may result in small-scale turbulence such as that indicated by the rising curve ($\overline{C} \simeq 4$ km/sec). But dynamic effects of this turbulence on the atmosphere are negligible.

With respect to the deviations from radiative equilibrium, the formula

$$F_{conv} = lv\left[\frac{3}{2}\frac{kT\rho}{\bar{\mu}m_H} + \alpha I\right]\left[\frac{1}{\overline{T}}\frac{d\overline{T}}{dh} - \frac{\Gamma_2 - 1}{\Gamma_2}\frac{1}{\overline{P}}\frac{dP}{dh}\right] \tag{6}$$

permits their magnitudes to be estimated, even though it is not strictly applicable to the case envisioned here. The fraction α of the ionization energy per unit volume that must be used is difficult to define. If it is very small and if it also assumes that the mean free path l is of the order of the depth of the ionization region, one finds that the average element velocity $\bar{v}$ must be very high (several hundred km/sec) in order for F_{conv} to become comparable to the radiative flux. If one takes $\alpha = 1/2$ and assumes that half of the hydrogen is ionized, $\bar{v}$ must still be of the order of 50 km/sec, that is, clearly higher than the maximum value of v_1 found above.

It follows, then, that on the average the deviations from radiative equilibrium must /1020

not be large and consist primarily of an excess of ultraviolet energy, resulting from recombination of hydrogen.

Our observations correspond, in general, to the layers of small optical depths, located above the photosphere which is formed in this mass of intertwined flows. In this region the elements move under the action of the impetus, acquired in deeper layers, and the gravity g. Thus they can be considered to be in free fall except for the slight opposing effects of a very low average pressure and the viscosity, which reduces g_e in each element to a very small value.

The complete discussion of such a hypothesis, combined with the theory of pulsations, would certainly cause many kinematic and dynamic difficulties. However, as each element carries away with it the momentum characteristic of its level of origin, if the deep layers are agitated by a pulsation, this should be reflected in the radial velocities V_r observed spectroscopically.

This average velocity V_r can be integrated to give an idea of the average atmosphere displacement. Conversely, its derivative would not have much meaning since the actual acceleration d^2r/dt^2 of each element remains very close to -g at any instant of time, which, according to Eq. (2) where P_t is negligible ($\overline{C} \simeq 4$ km/sec), provides good confirmation of the decrease of g_e to a very low value.

On the other hand, the observed radial velocity curve should be appreciably smoothed by the effect of averaging over time and space compared to the curve at a greater depth, and these two curves should exhibit a non-negligible phase shift between them.

With regard to explaining the variations of g_e, a much more elaborate theory would be required. Nevertheless, it can be noted that within the framework on this hypothesis the deep layers, exert, on the average, a thrust on the upper layers during the expansion process. If one assumes that this effect is at maximum at the mid-point of the expansion, dP/dr and consequently g_e must also achieve their maximum valueaat this time, which is in accordance with observation. During contraction, on the other hand, the /1021
deep layers disappear in some fashion under the atmosphere which falls, as a unit, more freely in the gravitational field, with g_e passing through a minimum at about the middle of this contraction period.

Can the possibilities, which this qualitative discussion has revealed, be confirmed by a more rigorous and quantitative analysis? In particular, what is the precise meaning of the supersonic velocities, the existence of which seems to be derivable both from observation as from theory, and what are the ensuing consequences for the structure and the dynamics of the outer layers? Although definitive answers to the questions would lead to a considerable modification of our concepts, it seems useful to go to the discussion of the compatibility of the hypothesis with other points of view.

4. ENERGY CONSERVATION

In order to change from one model to another, it is important to verify that we would not have to supply appreciable amounts of energy to the atmosphere at the expense of the radiation flux F or vice versa. Since in this region the generation of subatomic energy is zero and the radiation energy is very low, the energy conservation equation, ignoring the curvature, can be written as:

$$C_p T\left(\frac{1}{T}\frac{dT}{dt}-\frac{\gamma-1}{\gamma}\frac{1}{P}\frac{dP}{dt}\right)=-\frac{dF}{dm} \tag{6}$$

where γ can be set equal to 5/3. Having represented the variations of P and T, derived from the models by tracing the motion of a particle during one period, as a function of the phase, let us evaluate dT/dt and dP/dt graphically and calculate the dF/dm, given in Table IV, for the particle supporting the masses of 72, 135 and 181 grams, respectively.

TABLE IV. VALUE OF dF/dm ($\bar{F} \simeq 4.25\times10^{10}$ ergs/cm^2)

Phases	72	135	181
0,05	+0,155 10⁶	+0,258 10⁶	+0,423 10⁶
0,15	-0,015 10⁶	+0,075 10⁶	+0,231 10⁶
0,25	+0,020 10⁶	+0,030 10⁶	+0,041 10⁶
0,35	-0,066 10⁶	-0,153 10⁶	-0,125 10⁶
0,45	0,000	-0,024 10⁶	-0,053 10⁶
0,55	-0,384 10⁶	-0,898 10⁶	-0,352 10⁶
0,65	-2,084 10⁶	-1,346 10⁶	-1,491 10⁶
0,75	+1,157 10⁶	+1,273 10⁶	+1,105 10⁶
0,85	+0,003 10⁶	+0,051 10⁶	-0,203 10⁶
0,95	-0,340 10⁶	-0,416 10⁶	-0,535 10⁶

It is seen that the total maximum variation of the flux through the atmosphere (ΣdF /1022 /dm $\times$ Δm) remains less than $\bar{F}/100$ for all the phases. Therefore, based on this, there is no serious incompatibility since the numerical integration of the radiative equilibrium does not ensure flux constancy with a higher accuracy.

5. RADIAL VELOCITY OF A PARTICLE

One can assume that the velocities observed spectroscopically always correspond to the same optical level, say, for example $\tau = 0.3$. Since the mass of matter above this level varies appreciably, these velocities, regardless of hypotheses such as those discussed in paragraph 3, cannot characterize the motion of an element of the material. In order to estimate this velocity, let us consider the continuity equation in Lagrangian coordinates

$$-\frac{\partial v_r}{\partial r}=\frac{1}{\rho}\frac{d\rho}{dt}+\frac{2v_r}{r}. \tag{7}$$

Using the curves of Fig. 1, we have evaluated $(1/\rho)d\rho/dt$ for the usual three particles, yielding the results listed in Table V.

TABLE V.

Phases	$\frac{1}{\rho}\frac{d\rho}{dt}$, derived for one particle supporting			$\frac{1}{\rho}\frac{d\rho}{dt}$ average
	72 gr	135 gr	181 gr	
0,05	$-0,30\ 10^{-6}$	$-0,33\ 10^{-6}$	$-0,11\ 10^{-6}$	$-0,25\ 10^{-6}$
0,15	$-0,45\ 10^{-6}$	$-0,38\ 10^{-6}$	$-0,28\ 10^{-6}$	$-0,37\ 10^{-6}$
0,25	$-0,58\ 10^{-6}$	$-0,62\ 10^{-6}$	$-0,46\ 10^{-6}$	$-0,55\ 10^{-6}$
0,35	$-0,98\ 10^{-6}$	$-0,92\ 10^{-6}$	$-0,84\ 10^{-6}$	$-0,01\ 10^{-6}$
0,45	$-1,7\ 10^{-6}$	$-1,5\ 10^{-6}$	$-1,4\ 10^{-6}$	$-1,5\ 10^{-6}$
0,55	$-2,8\ 10^{-6}$	$-2,4\ 10^{-6}$	$-2,8\ 10^{-6}$	$-2,6\ 10^{-6}$
0,65	$-6,6\ 10^{-6}$	$-5,1\ 10^{-6}$	$-6,1\ 10^{-6}$	$-5,9\ 10^{-6}$
0,75	$+5,4\ 10^{-6}$	$+5,6\ 10^{-6}$	$+4,4\ 10^{-6}$	$+5,2\ 10^{-6}$
0,85	$+2,2\ 10^{-6}$	$+2,5\ 10^{-6}$	$+2,1\ 10^{-6}$	$+2,3\ 10^{-6}$
0,95	$+0,62\ 10^{-6}$	$+0,37\ 10^{-6}$	$+0,16\ 10^{-6}$	$+0,38\ 10^{-6}$

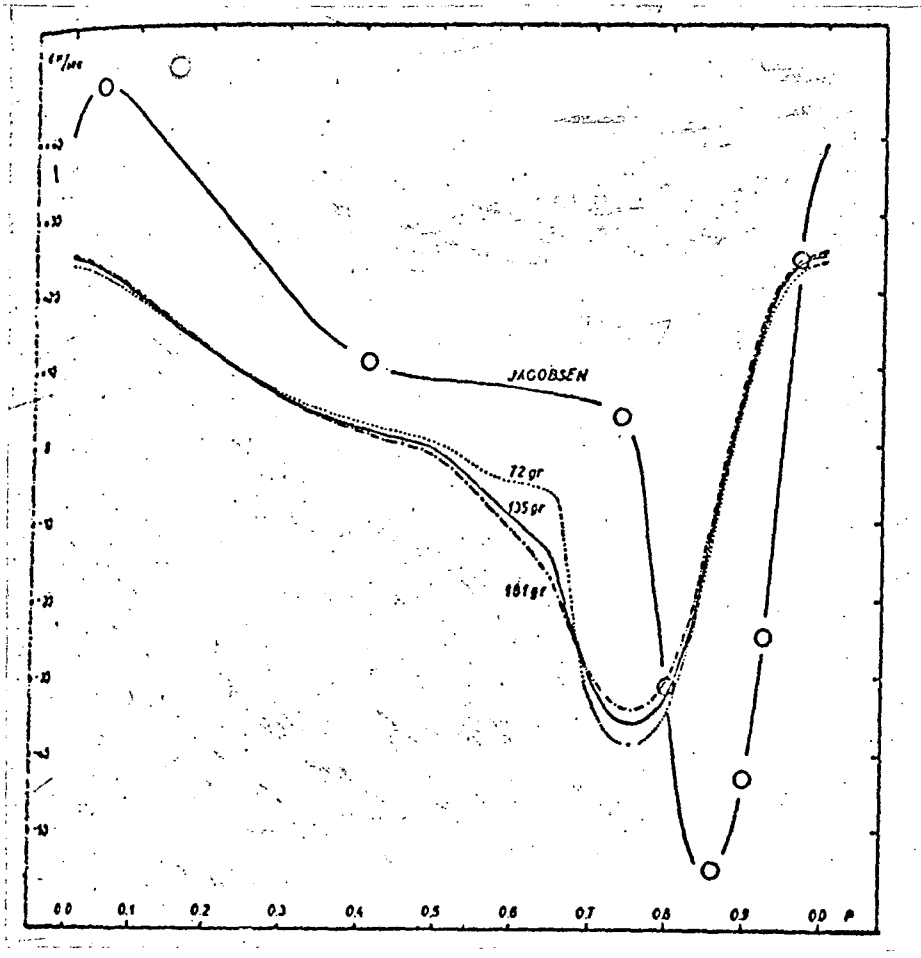

Fig. 5. Curves of the velocity dr/dt, calculated for three particles: dotted lines: particle supporting 72 grams, solid line: particle supporting 135 grams, dot-dash line: particle supporting 181 grams. The fourth curve (small circles) represents the radial velocity measurements made by Jacobsen on the absorption centers of the H and K lines.

Because of the low precision of this determination, we have adopted an average value /1023 for the three elements in each phase. With the term $2V_r/r$ determined from the observed radial velocity curve, Eq. (7) gives us an average value of the velocity gradient. The latter permits us, by using the distance between the optical level $\tau = 0.3$ and each of the particles, to determine the velocity of these particles in each of the phases considered. These results lead to Table VI and Fig. 5.

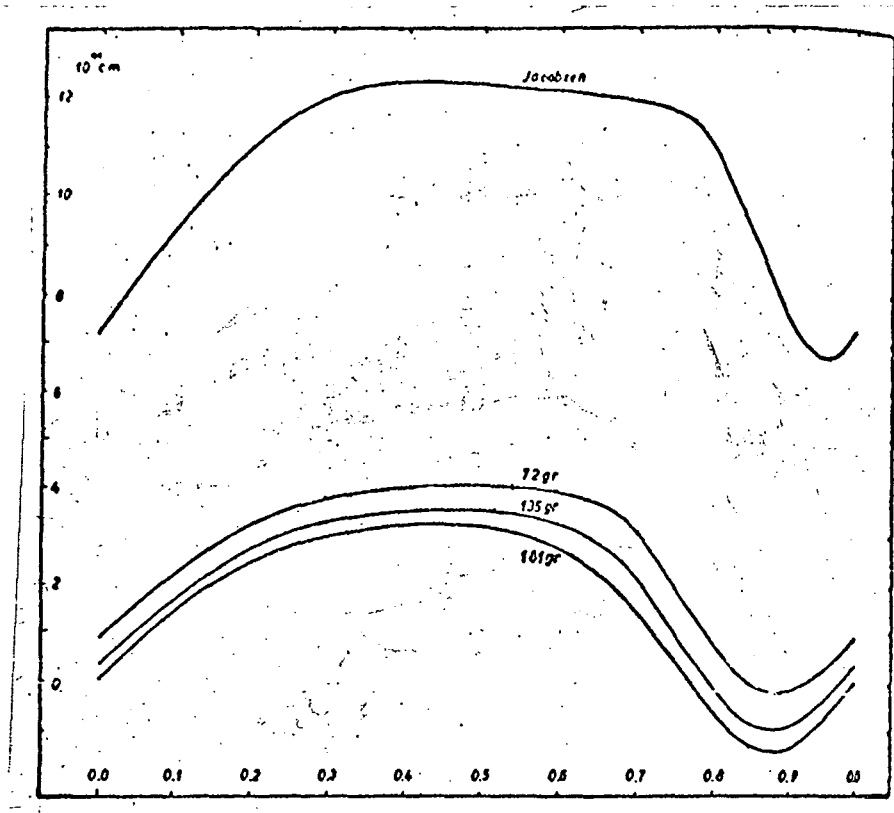

Fig. 6. Radius variation for different particles.

TABLE VI

	$-\frac{\partial v_r}{\partial r} = \frac{1}{\rho}\frac{d\rho}{dt} + \frac{2vr}{r}$	$\rightarrow \Delta r = +\Delta h = h_{\text{particle}} - h_{\tau=0,3}$			v_r of the particles		
		72 gr	135 gr	181	72 gr	135 gr	181 gr
0,00	+1,13 10^{-6}	-0,50 10^{11}	0,00	+0,30 10^{11}	+24,2	+24,9	+25,3
0,15	+0,35 10^{-6}	-0,73 10^{11}	-0,14 10^{11}	+0,17 10^{11}	+16,4	+16,7	+16,8
0,35	-0,78 10^{-6}	-0,92 10^{11}	-0,25 10^{11}	+0,10 10^{11}	+ 4,2	+ 3,7	+ 3,4
0,55	-3,01 10^{-6}	-1,44 10^{11}	-0,60 10^{11}	-0,22 10^{11}	- 3,2	- 5,7	- 6,8
0,65	-6,89 10^{-6}	-2,27 10^{11}	-1,10 10^{11}	+0,57 10^{11}	- 5,9	-13,9	-17,6
0,68	-1,14 10^{-6}	-2,44 10^{11}	-1,18 10^{11}	-0,63 10^{11}	-23,3	-24,8	-25,4
0,75	+3,65 10^{-6}	-1,44 10^{11}	-0,60 10^{11}	-0,22 10^{11}	-38,8	-35,7	-34,3
0,85	+1,60 10^{-6}	-0,42 10^{11}	-0,25 10^{11}	+0,10 10^{11}	-15,3	-14,2	-13,6
0,90	+1,74 10^{-6}	-0,78 10^{11}	-0,14 10^{11}	+0,17 10^{11}	+ 7,6	+ 8,7	+ 9,2

The most striking characteristic of these curves is surely the variation of their shape with depth. These are compatible with the results obtained in the study of the observed differential velocities in the atmosphere of η Aquilae [2] and especially with the conclusion that in phases 0.556 and 0.013, the absolute velocity in the two cases increases with the depth.

On the same figure, the curve joining the small circles represents best the radial velocities obtained by Jacobsen [14] from the absorption centers of the H and K lines. These velocities should characterize the motion of the boundary layers of the atmosphere. Although this curve is of little more than qualitative interest, it is interesting to note that it appears to be a very natural extrapolation of the curve for the outermost particle. We have also applied the correction factor 24/17 to Jacobsen's observations. /1025
However, it is probable that the correct factor is smaller and may be about 1. In this case the amplitude difference would be reduced considerably.

Taking the position of the element supporting 181 grams in phase 0.0 as the origin, /1026
one can, by integration of the curves of Fig. 4, obtain the relative displacements of the different elements represented in Fig. 6.

The primary effect seems to be that once the radius has reached its maximum length, the lower layers start to fall back faster than the upper layers until the point of minimum light (average radius) is reached; then the situation is reversed with the motion of the lower layers slowing down more rapidly than that of the upper layers. Thus, the deepest layers attain the expansion velocities more rapidly than the upper layers, a situation that continues until the pointsof maximum light and even a little beyond.

6. CONCLUSION /1027

The discussion of the variations, during the course of one period, of the properties of the models constructed to account for the observations at different phases has revealed no incompatibility with the theory of pulsations.

It appears that, provided the effective gravity g_e is suitably chosen, which in our models means a very low g_e that passes through a minimum when the light is a minimum, the atmosphere can be represented at each instant of time by a static model in radiative equilibrium that adopts itself to the energy flux to be transferred. The determination of g_e and of its variation is still a delicate problem, however, and merits a more detailed study, combining all possible sources of information.

The qualitative discussion of paragraph 3 suggests that the very high-rate convection flows from the hydrogen instability zone can distend the atmosphere (which remains, however, essentially in radiative equilibrium) well beyond its normal dimensions, with the effective gravity g_e being reduced to a very low value. Some of the consequences of such a hypothesis for the theory of pulsations have been discussed qualitatively while ignoring all supersonic phenomena (which can be important).

REFERENCES

1. J. Grandjean and P. Ledoux, Ann. Astr., 17, 161, 1954.
2. J. Grandjean, Mem. Ac. Roy. Sc. Belgique, in press.

3. W. S. Adams, M. Schwarzschild and B. Schwarzschild, Ap. J., 108, 207, 1948.
4. A. Pannekoek and J. M. Reesinck, B. A. N., 3, 47, 1925.
5. A. Pannekoek, B. A. N., 8, 175, 1937.
6. A. Pannekoek and F. B. van Albada, Publ. Astr. Inst. Univ., Amsterdam, No. 6, part 2, 2, 1946.
7. Th. Walhaven, Publ. Astr. Inst. Univ., Amsterdam, No. 8, 1948.
8. A. Pannekoek, "Zeeman Congress", Physica, XII, 761, 1946.
9. R. Canavaggia and J. C. Pecker, "Fundamental Principles of Star Classification", C. N. R. S., 1955, p. 169.
10. C. A. Whitney, Thesis, Harvard University, April 1955.
11. D. Koelbloed, Publ. Astr. Inst. Univ., Amsterdam, No. 10, 1953.
12. P. Dumezil-Curien, Ann. Astr., 17, 197, 1954.
13. See for example: D. H. Menzel, "Zeeman Congress", Physica, XII, 768, 1946. A. McKellar and G. J. Odgers, Transactions of the I. A. U., VIII, 825, 1952.
14. T. S. Jacobsen, P. A. S. P., 64, 308, 1952.

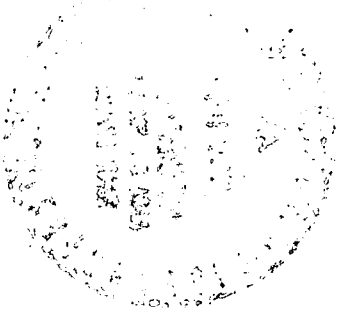

Translated for the National Aeronautics and Space Administration by Scripta Technica, Inc. NASW 2036.